Protective actions of des-acylated ghrelin on brain injury and blood-brain barrier disruption after stroke in mice

Jacqueline M. Ku[1], Mohammadali Taher[1], Kai Yee Chin[1], Tom Barsby[1], Victoria Austin[1], Connie H. Y. Wong[2], Zane B. Andrews[3], Sarah J. Spencer[1] and Alyson A. Miller[1*]

[1]*Cerebrovascular and Stroke Laboratory, School of Health and Biomedical Sciences, RMIT University, Melbourne, Victoria 3083, Australia*

[2]*Centre for Inflammatory Diseases, Department of Medicine, Monash Medical Centre, Monash University, Melbourne, Victoria 3168, Australia,*

[3]*Department of Physiology, Monash University, Melbourne, Victoria 3800, Australia*

[*]Author for correspondence and for reprint requests:

Doctor Alyson A. Miller

School of Health and Biomedical Sciences

RMIT University

Bundoora

Australia

Telephone: +61 3 9925 7589

Fax: +61 3 9927 7063

E-mail: alyson.miller@rmit.edu.au

Abstract

The major ghrelin forms, acylated ghrelin and des-acylated ghrelin, are novel gastrointestinal hormones. Moreover, emerging evidence indicates that these peptides may have other functions including neuro- and vaso- protection. Here, we investigated whether post-stroke treatment with acylated ghrelin or des-acylated ghrelin could improve functional and histological endpoints of stroke outcome in mice after transient middle cerebral artery occlusion. We found that des-acylated ghrelin (1 mg/kg) improved neurological and functional performance, reduced infarct and swelling, and decreased apoptosis. In addition, it reduced BBB disruption *in vivo* and attenuated the hyper-permeability of mouse cerebral microvascular endothelial cells after oxygen glucose deprivation and reoxygenation (OGD + RO). By contrast, acylated ghrelin (1 mg/kg or 5 mg/kg) had no significant effect on these endpoints of stroke outcome. Next we found that des-acylated ghrelin's vasoprotective actions were associated with increased expression of tight junction proteins (occludin and claudin-5), and decreased cell death. Moreover, it attenuated superoxide production, Nox activity, and expression of 3-nitrotyrosine. Collectively, these results demonstrate that post-stroke treatment with des-acylated ghrelin, but not acylated ghrelin, protects against ischemia/reperfusion-induced brain injury and swelling, and BBB disruption by reducing oxidative and/or nitrosative damage.

Summary statement

Stroke is a leading cause of death, but treatments are limited. This experimental study reveals that the hormone ghrelin powerfully protects the brain and its blood vessels against injury after stroke, raising the possibility that it could be exploited therapeutically.

Short title

Des-acylated ghrelin protects against stroke.

Keywords

Ischemia, reperfusion, ghrelin, neuroprotection, blood-brain barrier.

Abbreviations list

Blood-brain barrier (BBB); ghrelin O-acyltransferase (GOAT); growth hormone secretagogue receptor 1a (GHSR1a); oxygen glucose deprivation and reoxygenation (OGD +

RO); reactive oxygen species (ROS); reactive nitrogen species (RNS); recombinant tissue plasminogen activator (rt-PA); regional cerebral blood flow (rCBF); transient middle cerebral artery occlusion (tMCAo).

Clinical perspectives

- Ischemic stroke is a leading cause of mortality and long-term disability, but treatment options are limited. The major ghrelin forms, acylated ghrelin and des-acylated ghrelin, are novel gastrointestinal hormones. Moreover, recent evidence indicates these peptides may have neuroprotective and vasoprotective actions, and thus may protective actions in ischemic stroke.
- In this study we tested whether the peptides could mediate protection in a clinically relevant mouse model of ischemic stroke.
- Our findings reveal protective actions of des-acylated ghrelin when administered shortly after induction of reperfusion, which involve a previously unrecognized beneficial effect on blood-brain barrier integrity. By contrast the acylated form was without effect. Thus, this study sheds light on the potential of des-acylated ghrelin or longer acting analogues as novels therapeutic agents for ischemia/reperfusion-induced injury. These findings may prove to be all the more crucial when we consider that the production of this peptide may be reduced after stroke.

Introduction

Pharmacological treatment of ischemic stroke mainly relies on the use of recombinant tissue plasminogen activator (rt-PA). However, it is only administered to a small proportion of stroke patients due to its propensity to increase the risk of hemorrhage and edema if delayed >4.5 hours after stroke onset. Also, even if rt-PA-induced or spontaneous restoration of blood flow occurs, reperfusion often exacerbates brain injury. Thus, there is a pressing need for novel agents that protect against not only ischemia but also reperfusion injury. A burst of reactive oxygen and nitrogen species generation (ROS & RNS; commonly referred to as oxidative/nitrosative stress) is an important mechanism of neuronal cell death after ischemia and reperfusion (1, 2). Moreover, such mechanisms also contribute to blood-brain barrier (BBB) disruption after ischemia and reperfusion, as well as dysfunction of arteries upstream of the BBB (3, 4). There is a growing appreciation of the contribution of these vascular changes to brain injury and edema, and thus the importance of protecting the cerebral endothelium as part of an effective stroke therapy (5).

Ghrelin is a 28 amino acid peptide hormone produced primarily by the stomach. In the plasma, ghrelin circulates in at least two distinct forms, acylated ghrelin and des-acylated ghrelin. Post-translational addition of a medium-chain fatty acid by the enzyme ghrelin O-acyltransferase (GOAT) produces the acylated form of ghrelin (6). Acylated ghrelin is a metabolic hormone that stimulates appetite and regulates energy expenditure largely through its actions on the growth hormone secretagogue receptor 1a (GHSR1a) expressed in the hypothalamus and pituitary gland (7). Des-acylated ghrelin is the most abundant circulating ghrelin form, but it does not bind or activate GHSR1a at physiological concentrations (8). Recent evidence suggests that it may have opposing metabolic actions to acylated ghrelin (9). However, to date, a receptor for des-acylated ghrelin has not been identified. Interest in these peptides has intensified over the past decade with the realization that they may have diverse actions beyond their roles in metabolism (7). Acylated ghrelin signaling in the brain promotes learning and memory, protects against neurodegeneration (e.g. in Parkinson's disease) by activating UCP2-dependent mitochondrial mechanisms, and has antidepressant and anxiolytic effects (7, 10). Furthermore, acylated ghrelin (11-13) and des-acylated ghrelin (11) reduce brain injury in rat models of cerebral ischemia and reperfusion when administered before induction of ischemia, and reduce apoptotic cell death of neurons *in vitro* (14, 15). Most importantly, however, it remains to be tested whether these peptides are also protective when

given after stroke induction, which represents a more clinical relevant scenario. Notably, des-acylated ghrelin may also have beneficial effects on the cerebral endothelium after ischemia and reperfusion. Indeed, this ghrelin form suppresses superoxide levels in mouse cerebral vessels by inhibiting the Nox-NADPH oxidases (16), which are major contributors to oxidative-induced BBB disruption after stroke (17, 18).

The aims of this study were, therefore, to firstly test the effect of acylated ghrelin and des-acylated ghrelin on outcome following transient middle cerebral artery occlusion in mice, when administered after induction of cerebral reperfusion. Secondly, we examined whether the peptides can inhibit BBB disruption by measuring their effects on BBB permeability *in vivo*, and also cerebral endothelial permeability after oxygen glucose deprivation (OGD) and reoxygenation (RO) *in vitro*.

Materials and Methods

This study followed the ARRIVE Guidelines. All experimental procedures were conducted in accordance with the NHMRC guidelines for the care and use of animals for research and were approved by the RMIT University Animal Ethics Committee. A total of 178 male [22 excluded, see below], 8-12 week old C57Bl6/J mice were obtained from the Animal Resources Centre (Australia). Mice had access to water and standard chow *ab libitum*, and were housed under a 12:12 light:dark cycle in a SPF facility. Mice were randomly assigned to treatment groups by an investigator not performing surgical procedures or post-surgery analyses, and an investigator blinded to the treatment groups performed post-surgery analyses. In total, 22 stroke mice were excluded from the study which occurred when: (1) there was an inadequate (<70%) reduction in regional cerebral blood flow (rCBF) during the ischemic period or inadequate (>80%) increase within the first 10 min of reperfusion (n=5); (2) technical complications arose during surgery (e.g. loss of >0.2 mls of blood, n=2; the occluding clamp on the common carotid artery was in place for ≥5 min, n=1); or (3) they died or had to be euthanized (according to clinical severity score) prior to the end of the reperfusion period (n=6 vehicle-treated mice; n=5 acylated ghrelin-treated; and n=3 des-acylated ghrelin-treated).

Focal cerebral ischemia and reperfusion

Mice were anesthetized between 7 am and 11 am with a mixture of ketamine (150 mg/kg, i.p.) and xylazine (10 mg/kg, i.p.). Body temperature was maintained at 37ºC with a heat lamp throughout the procedure and until mice regained consciousness. Focal cerebral ischemia and reperfusion was performed by transient intraluminal filament-induced middle cerebral artery occlusion (tMCAo) as previously described (19-21). Regional cerebral blood flow (rCBF) in the area of the cortex supplied by the MCA (~2 mm posterior and 5 mm lateral to bregma) was monitored and recorded prior to the induction of cerebral ischemia, during ischemia, and during the first 10 min of reperfusion using trans-cranial laser-Doppler flowmetry. For sham surgery, the right external carotid artery and common carotid artery were visualized, but the filament was not inserted. After mice had recovered from anaesthesia, they were housed in individual cages. Mice were monitored hourly for a minimum of 8 hours (during 8 am - 6 pm) post-surgery and the following morning (7 am) using our monitoring protocol and clinical signs severity scoring system (approved by our

ethics committee). At the end of the experiment, mice were euthanized with an overdose of isoflurane followed by decapitation.

Ghrelin treatment regime

Mice received three injections of vehicle (0.9% saline, i.p.), acylated ghrelin (1 or 5 mg/kg, i.p.), or des-acylated ghrelin (1 mg/kg, i.p.). Doses were administered at the time of reperfusion, and at 8 and 16 h of reperfusion. Doses were calculated from published work showing neuroprotective effects of these peptides *in vivo* when administered prior to stroke (11-13), and our work showing protective actions of des-acylated ghrelin on cerebral arteries (16). Acylated ghrelin is known to stimulate food intake, which could in turn improve the well-being and thus influence the recovery of mice. Thus, in a small cohort of mice we measured food intake overnight for 3 days (baseline) prior to sham or stroke surgery and on the night following surgery.

Neurological deficit scoring and functional impairment test

Neurological assessment was performed 24 h after sham or stroke surgery using a five-point scoring system: 0 = normal motor function; 1= flexion of torso and contralateral forelimb when lifted by the tail; 2 = circling to the contralateral side when held by the tail on a flat surface with normal posture at rest; 3 = leaning on the contralateral side at rest; 4 = no spontaneous movement at rest or uncontrolled circling (20). After neurological assessment and a rest period (10 min), a hanging wire test was performed, as previously described (4, 20).

Quantification of cerebral infarct and edema volumes

Cerebral infarct and edema volumes were evaluated at 24 h after stroke surgery, as previously described (4, 20). Briefly, brains were coronally sectioned (30 μm thickness; 420 μm apart) and then stained with 0.1% thionin to delineate the infarct. Total infarct volume was quantified using ImageJ image analysis software, correcting for brain edema, as previously described (4, 20).

Measurement of cell death using TUNEL

The TUNEL method was used to quantify cell death in brain sections (10 μm) of mice 24 h after stroke, as per manufacturer instructions (*In Situ* Cell Detection Kit, Roche). Infarcts were located on each section by comparing to corresponding thionin-stained sections. The

number of TUNEL-positive cells was then counted in both infarct and peri-infarct regions of the ischemic hemisphere. The peri-infarct was assessed as any region outside the infarct in the ischemic hemisphere that displayed TUNEL positive immunoreactive staining (20). Three sections were analysed per mouse and the total number of TUNEL-positive cells averaged.

Expression levels of cleaved caspase-3

Western blotting was used to measure expression levels of the apoptotic protein cleaved caspase-3 in ischemic/right cerebral hemispheres of mice 24 h after sham or stroke surgery using methods similar to those previously reported (4, 20). Rabbit polyclonal anti-cleaved caspase-3 (1:1000) and anti-β-actin (1:5000) primary antibodies were used (both from Cell Signaling Technology). Immunoreactive band intensities were normalized to intensity of corresponding bands for β-actin and expressed as fold-change relative to sham.

RT-PCR

RT-PCR was used to measure GHSR1a mRNA expression levels in: (1) ischemic/right cerebral hemispheres of control mice (received no surgical intervention), and of mice 24 h after sham or stroke surgery (vehicle and acylated ghrelin-treated mice). It is known that des-acyl ghrelin does not bind to nor activate GHSR1a (8, 22). Thus, any protective actions of des-acyl ghrelin after stroke will not mediated through GHSR1a. As such, we did not assess GHSR1a mRNA expression levels in brains from des-acylated ghrelin-treated mice; (2) middle cerebral arteries (MCA) of sham and stroke mice; and pituitary of control mice (positive control); and (3) bEnd.3 cells cultured under normoxic or OGD + RO conditions (see below), as previously described (16). QuantiFast SYBR® Green primers were used (GHSR1a, Cat no. QT00138439; 18s, Cat no. QT02448075). Data were normalized to ribosomal 18s and represented relative to expression levels in either sham (brain) or pituitary gland (cerebral arteries and cells) using the $2^{-\Delta\Delta Ct}$ method.

Assessment of blood-brain barrier disruption *in vivo*

4 mL/kg of 2% Evan's blue was injected into the tail vein of mice 21 h after sham or stroke surgery. After 3 h, mice were euthanized by inhalation of isofluorane and transcardially perfused with 0.9% saline. The ischemic/right and contralateral/left hemispheres were then homogenized in *N,N*-dimethylformamide, incubated overnight at 55°C, and centrifuged. Supernatants were collected and absorbance read in triplicate, alongside a standard curve of 0–15,000 ng/mL Evan's blue, using a BMG Clariostar plate reader (620 nm excitation, 680

nm emission). The amount of Evan's blue per ischemic/right hemispheres (micrograms) was expressed as a ratio of levels in contralateral/left hemispheres.

Oxygen glucose deprivation and reoxygenation of bEnd.3 cells

Mouse microvascular cerebral endothelial cells (bEnd.3 cells; ATCC CRL-2299) were grown in culture media (Dulbecco's modified Eagle's medium [DMEM] containing 10% fetal bovine serum [FBS]) at 37°C in a humidified 5% CO_2 atmosphere. Cells were passaged every 3-4 days. Culture media was changed after 24 h of passaging and every 2 days thereafter. Experiments were performed with cells from passages 24 to 34.

bEnd.3 cells were washed twice with OGD media composed of glucose- and serum- free DMEM media (Invitrogen) pre-equilibrated for 5 min with 100% N_2. Cells were then transferred to a humidified hypoxia chamber linked to a digital oxygen controller (0.3% oxygen, Biospherix) filled with 95% N_2, 5% CO_2 and left to incubate for 1 h at 37°C. Cells were then washed twice with glucose-containing DMEM media (oxygenated with air), and incubated for a further 23 h in glucose-containing DMEM media (no serum) in a humidified normoxic incubator (5% CO_2 atmosphere) at 37°C. For normoxic controls, bEnd.3 cultures were incubated for the same duration of time as the OGD + RO cells in glucose-containing, serum-free medium (equilibrated with air) at 37°C (5% CO_2 atmosphere).

Measurement of paracellular permeability in bEnd.3 cells after OGD + RO

To measure endothelial cell paracellular permeability, the passage of FITC-dextran (70 kDa) across bEnd.3 cells monolayers was measured after exposure to normoxic conditions and OGD + RO. Cells were treated with either vehicle (0.9% saline) acylated ghrelin, or des-acylated ghrelin (10 nmol/L) at the time of RO (post-treatment protocol). Moreover, we tested the effect of des-acylated ghrelin when administered 24 h prior to OGD (pre-treatment protocol). 10 nmol/L was selected based on our published work showing protective actions of des-acylated ghrelin on the cerebral vasculature (16).

bEnd.3 cells were seeded at a density of $5x10^4$ cells/well in DMEM media (10% FBS) onto the upper 'apical' chamber of transwell inserts (0.4 μm average pore size, ThinCerts™) fitted into 24-well culture plates. Following normoxic or OGD + RO exposure, inserts were transferred into new wells of 24-well culture plates containing pre-warmed Krebs-HEPES buffer (pH=7.4). FITC-dextran (1 mg/mL) was then added to the upper chamber and left to

incubate for 60 min at 37°C. Inserts were then removed from the wells and samples taken from the lower chamber and transferred into a 96-well black plate. Fluorescence intensity was then measured using the BMG Clariostar plate reader at an excitation (492 nm) and emission (518 nm) wavelength. Fluorescence intensity was calculated as fold-change relative to normoxic controls.

Measurement of tight junction protein expression in bEnd.3 cells after OGD + RO

Western blotting was used to measure expression levels of tight junction proteins occludin, claudin-5, and ZO-1, in bEnd.3 cells exposed to normoxic conditions or OGD + RO, using methods similar to those previously reported (23). Cells were treated with either vehicle (0.9% saline) or des-acylated ghrelin (10 nmol/L) at the time of RO. Mouse monoclonal anti-occludin and anti-claudin-5, rabbit polyclonal anti-ZO-1 (Invitrogen; 1:1000 for all antibodies), and anti-β-actin (1:5000, Cell Signaling) primary antibodies were used. Immunoreactive band intensities were normalized to intensity of corresponding bands for β-actin and expressed as fold-change relative to normoxic controls.

Immunofluorescence for ZO-1 and 3-nitrotyrosine in bEnd.3 cells after OGD + RO

bEnd.3 cells were seeded onto glass coverslips in culture media (DMEM media with 10% FBS). 2 days post-confluence, cells were exposed to normoxic conditions or OGD + RO (treated with either vehicle [0.9% saline] or des-acylated ghrelin [10 nmol/L] at the time of RO), fixed with 4% paraformaldehyde, washed with 0.01 mol/L PBS (3 x 10 min), and then incubated with 10% goat serum (30 min). Immunofluorescence was then performed using polyclonal rabbit anti-ZO-1 (1:300, Zymed Laboratories) or polyclonal rabbit anti-3-nitrotyrosine (1:350, Abcam) primary antibodies, and goat anti-rabbit AlexFluoro594 (ZO-1; 1:500, Invitrogen) or AlexFluoro488 (3-nitrotyrosine; 1:350, Invitrogen) secondary antibodies. Cells were counterstained with Hoescht 33342 solution (1:500, Sigma). For 3-nitrotyrosine, 5 fields of view were randomly selected per coverslip and semi-quantitative analysis of fluorescence intensity performed as previously described (24), and appropriate negative and positive controls were performed. Values were then expressed as fold-change relative to normoxic controls.

Measurement of cell viability of bEnd.3 cells and cleaved caspase-3 expression after OGD + RO

Cell viability of bEnd.3 cells (exposed to normoxic or OGD + RO conditions) was assessed using the MTS assay (Promega). Cells were treated with either vehicle (0.9% saline) or des-acylated ghrelin (10 nmol/L) at the time of RO or for 24 hours prior to OGD + RO (pre-treatment protocol). Absorbance was measured detected at 490 nm using a BMG Clariostar plate reader. Mean absorbance of cells exposed to OGD + RO were expressed as fold-change relative to the absorbance of normoxic cells. Western blotting was used to measure expression levels of cleaved caspase-3 in bEnd.3 cells exposed to normoxic conditions or OGD + RO, using methods similar to those previously reported (23).

Measurement of superoxide production by bEnd.3 cells after OGD + RO

Basal and angiotensin II-stimulated superoxide production by bEnd.3 cells (exposed to normoxic or OGD + RO conditions) was assessed using either L-012 (100 μmol/L)-enhanced chemiluminescence or ethidium/oxyethidium fluorescence (dihydroethidium; 10 μmol/L), as previously described (4, 25). Cells exposed to OGD + RO were treated with either vehicle or des-acyl ghrelin (10 nmol/L) at the time of RO. We have previously demonstrated that superoxide dismutase (SOD) or Tempol abolishes the L-012-chemiluminescence signal detected from vascular preparations, implying that L-012 detects superoxide and not other ROS (26). To confirm that superoxide was the major ROS detected by DHE, bEnd.3 cells were treated with PEG-SOD (500 U/mL) at the time of RO. For L-012 experiments, superoxide counts were measured for 60 minutes and background counts were then subtracted. Values were then expressed as percentage relative to normoxic controls.

Data and statistical analysis

All results are presented as mean ± SEM and $P<0.05$ was considered statistically significant. Statistical analyses were performed using GraphPad Prism version 6 (GraphPad Software Inc., USA). Statistical comparisons between treatment groups were performed using either a Student's unpaired *t* test or 1-way ANOVA with a Dunnet's multiple comparisons post-hoc test. Mann-Whitney U-test was used for nonparametric data.

Drugs and their sources

Drugs and their sources are: acylated ghrelin (SC1357; Polypeptide Laboratories, France); des-acylated ghrelin (SC1483; Polypeptide Laboratories, France); and all other drugs

(Sigma). All ghrelin-related peptides were dissolved in 0.9% saline. All other drugs were dissolved in either Krebs-HEPES buffer or distilled water.

Results

Degree of hypoperfusion, mortality, and food intake

Following insertion of the monofilament, rCBF was reduced by ~75 % and increased upon removal to a similar extent in groups (P>0.05, Figure 1A). In sham-operated mice, rCBF remained at ~100% for the duration of the monitoring period (Figure 1A). Mortality during the reperfusion period was 6/48 (12%) of vehicle-treated mice, 5/44 (11%) of acylated ghrelin-treated mice, and 3/38 (8%) of des-acylated ghrelin mice. Overnight food intake was reduced in vehicle-treated stroke mice relative to baseline and sham-operated mice (Table 1, P<0.05, 1-way ANOVA with a Dunnett's post-hoc test). Treatment with acylated ghrelin had no effect on food intake in mice after stroke (Table 1, P>0.05 vs. vehicle-treated stroke mice, unpaired t-test), but increased food intake in sham-operated mice relative to baseline (Table 1, P<0.05, unpaired t-test).

Des-acylated ghrelin improves stroke outcomes

Post-stroke treatment of mice with 1 mg/kg acylated ghrelin had no significant effect on neurological deficit scores, hanging grip times, or infarct and edema volume relative to vehicle-treated mice (Figure 1B-E). Similarly, mice treated with a higher dose of acylated ghrelin (5 mg/kg) displayed no improvement in neurological deficit, hanging grip times (5 mg/kg acylated ghrelin: 29 ± 6 vs. vehicle: 30 ± 9 s vs., P>0.05, unpaired t test, n=9), or infarct and edema volumes (Figures 1F &1G). By contrast, post-stroke treatment with 1 mg/kg des-acylated ghrelin significantly improved neurological score and hanging grip time, and reduced both infarct and edema volume by >50% (Figures 1B-E, P<0.05).

Des-acylated ghrelin reduces apoptosis after stroke

In vehicle-treated mice, there was an abundance of TUNEL-positive cells in both peri-infarct (149 ± 36) and infarct brain regions (4814 ± 704, Figure 2A). Post-stroke treatment with 1 mg/kg acylated ghrelin had no significant effect on the number of TUNEL-positive cells in both peri-infarct (111 ± 16) and infarct (4187 ± 468) regions relative to vehicle-treated mice. However, in mice treated with 1 mg/kg des-acylated ghrelin, there were ~70% fewer TUNEL-positive cells in peri-infarct regions (46 ± 9, P<0.05), and there was also a trend for less TUNEL-positive cells in infarct regions (2720 ± 706 TUNEL-positive cells, P=0.08). Virtually no TUNEL-positive cells were observed in the contralateral hemisphere of brains from stroke mice (Figure 2A).

Western blot analysis indicated that expression of cleaved caspase-3 (17 kDa subunit) was significantly increased in ischemic hemispheres of vehicle-treated mice relative to sham mice ($P<0.05$, Figure 2B). Consistent with our infarct and TUNEL data, expression levels of cleaved caspase-3 in ischemic hemispheres of acylated ghrelin-treated mice were comparable to that of vehicle-treated mice ($P<0.05$, Figure 2B). By contrast, expression levels in ischemic hemispheres of des-acylated ghrelin-treated mice (1 mg/kg) were significantly lower than in vehicle-treated mice ($P<0.05$, Figure 2C) and comparable to levels in sham mice ($P>0.05$). Expression levels of the 19 kDa subunit of cleaved caspase-3 were similar between sham (0.35 ± 0.04, relative intensity to β-actin), vehicle-treated (0.44 ± 0.04), and des-acylated ghrelin-treated mice (0.36 ± 0.05; $P>0.05$).

Effect of stroke on GHSR1a mRNA expression

Using RT-PCR, we next tested whether acylated ghrelin's lack of effect on stroke outcome relates to down-regulation of its receptor, GHSR1a, in the ischemic hemisphere. Expression levels of GHSR1a mRNA in the brain were similar between control and sham-operated mice, indicating that anaesthesia/surgery *per se* does not affect GHSR1a expression (Figure 3A). In vehicle-treated stroke mice, GHSR1a mRNA expression was significantly lower relative to control and sham mice ($P<0.05$), whereas levels were not decreased in mice treated with acylated ghrelin (1 mg/kg). Thus, post-stroke treatment with acylated ghrelin prevents down-regulation of its receptor in the ischemic brain.

We have previously reported that although GHSR1a mRNA is expressed at low levels in mouse cerebral arteries, it is not expressed at the protein level(16). Similarly, we found here that GHSR1a mRNA expression in cerebral arteries of sham-operated mice was very low (~22-fold lower relative to pituitary [positive control]; $P<0.05$, Figure 3B), and expression levels were negligible in cerebral arteries of stroke mice (~14-fold lower relative to sham-operated, $P<0.05$). Similarly, GHSR1a mRNA expression was negligible in bEnd.3 cells cultured under either normoxic or OGD conditions (~2200-fold lower relative to pituitary, $P<0.05$, data not shown). Thus, acylated ghrelin is unlikely to mediate direct effects on the mouse cerebral endothelium due to the lack of GHSR1a.

Des-acylated ghrelin reduces BBB disruption

There was marked extravasation of Evan's blue into ischemic hemispheres of vehicle-treated mice, indicative of increased BBB permeability and thus BBB disruption (Figure 4A,

P<0.05). Post-stroke treatment of mice with acylated ghrelin (1 mg/kg) had no significant effect on Evans's blue leakage relative to vehicle-treated mice, whereas des-acylated ghrelin (1 mg/kg) reduced leakage by ~80% (Figure 4A, *P*<0.05).

Acylated ghrelin (10 nmol/L) had no effect on paracellular hyper-permeability of bEnd.3 exposed to OGD + RO (Figure 4B). By contrast, des-acylated ghrelin (10 nmol/L) attenuated hyper-permeability of bEnd.3 cells. Specifically, post-treatment (i.e. at the time of RO) decreased the passage of FITC-dextran across bEnd.3 monolayers by ~30% relative to vehicle-treated cells (Figure 4B, *P*<0.05). Similarly, pre-treatment (i.e. 24 h before OGD) decreased the passage of FITC-dextran (normoxic: 5237 ± 142, OGD + RO vehicle-treated: 20409 ± 109, OGD + RO des-acylated ghrelin-treated: 15072 ± 189, RFU, P<0.05, n=6).

Effect of des-acylated ghrelin on tight junction protein expression in bEnd.3 cells

Western blot analysis showed that expression of occludin and ZO-1 were reduced in vehicle-treated cells after OGD + RO relative to normoxic (*P*<0.05, Figure 5A and B). The decline in occludin levels was virtually prevented by des-acylated ghrelin (10 nmol/L; post-treatment, *P*<0.05, Figure 5A); however, it had no significant effect on ZO-1 expression (Figure 5B). Expression of claudin-5 was unchanged in vehicle-treated cells after OGD + RO (*P*>0.05, Figure **5C**). Treatment with des-acylated ghrelin significantly increased expression levels (*P*<0.05, Figure **5C**).

In accordance with our Western blot data, immunofluorescence staining for ZO-1 appeared to be less intense in vehicle-treated cells. Also, ZO-1 immunoreactivity was more discontinuous along the cell membrane than normoxic controls, which might suggest re-distribution of this protein (Figure 5D). In cells treated with des-acylated ghrelin, ZO-1 immunoreactivity was also less in intense; however, there appeared to be a more continuous alignment of ZO-1 to the cell membrane.

Effect of des-acylated ghrelin on viability and caspase-3 expression in bEnd.3 cells

After exposure to OGD + RO, the viability of vehicle-treated bEnd.3 cells was decreased by >20% relative to normoxic controls (Figure 5E, *P*<0.05). Treatment of cells with des-acylated ghrelin significantly increased cell viability relative to vehicle-treated cells (*P*<0.05).

Western blot analysis revealed a significant increase in expression levels of cleaved caspase-3 (17 kDa subunit) in vehicle-treated and des-acylated ghrelin-treated cells exposed to OGD +

RO (P<0.05, Figure 5F), and levels were comparable between vehicle- and des-acylated ghrelin treated cells. The 19 kDa subunit was undetectable in either normoxic or OGD + RO cells.

Des-acylated ghrelin attenuates superoxide levels, Nox activity, and 3-nitrotyrosine in bEnd.3 cells

After exposure to OGD + RO, basal superoxide production by bEnd.3 cells was ~2.5-fold greater than levels generated by normoxic cells, as measured by L-012-enhanced chemiluminescence (P<0.05, Figure 6A). However, in des-acylated ghrelin-treated cells, superoxide production was decreased by ~40% (P<0.05). We also found that ethidium/oxyethidium fluorescence appeared to be less intense in cells treated with des-acylated ghrelin relative to vehicle-treated (Figure 6B). PEG-SOD also appeared to significantly reduce fluorescence intensity, confirming that superoxide was the major ROS detected by DHE.

Angiotensin II is known to increase superoxide production by cerebral vessels by activating the Nox-NADPH oxidases (Nox1- and Nox2-containing isoforms) and is commonly used to assess Nox activity in vessel preparations and vascular cells (16, 27, 28). Acylated ghrelin (0.1-10 nmol/l) had no significant effect on Nox activity, which is also consistent with our findings in intact mouse cerebral vessels (16) (Figure 6C). Similar to its inhibitory effect on Nox activity in intact mouse cerebral arteries (16), des-acylated ghrelin (1-10 nmol/L) markedly reduced angiotensin II-stimulated superoxide generation (~50 %), and thus Nox activity, in bEnd.3 cells exposed to normoxic conditions (Figure 6D, P<0.05). After exposure to OGD + RO, angiotensin II-stimulated superoxide generation was increased ~2-fold in vehicle-treated bEnd.3 cells relative to normoxic controls (P<0.05, Figure 6E). Moreover, treatment with des-acylated ghrelin prevented this increase in Nox activity such that superoxide levels were comparable to levels in normoxic controls (P>0.05).

Using immunofluorescence and semi-quantitative analysis, we found that 3-nitrotyrosine expression (marker of protein nitration by peroxynitrite) was increased by ~2-fold in bEnd.3 cells after OGD + RO (P<0.05, Figure 7). Importantly, treatment with des-acylated ghrelin significantly reduced expression levels (P<0.05, Figure 7).

Discussion

Our data demonstrate that the des-acylated form of ghrelin improves functional and neurological deficit, and reduces the degree of injury, apoptosis, and swelling when administered to mice shortly after induction of reperfusion. By contrast, at the two doses we tested, acylated ghrelin fails to improve these end-point measures of stroke outcome. This study also reveals that the beneficial effect of des-acylated ghrelin relates, at least in part, to its ability to protect against BBB disruption. Moreover, this effect occurs in association with reduced ROS/RNS production and Nox activity, inferring des-acylated ghrelin enhances BBB integrity by reducing oxidative/nitrosative damage.

When administered prior to or at the immediate onset of ischemia, acylated ghrelin reduces brain injury in rat models of ischemia and reperfusion through anti-apoptotic and anti-inflammatory mechanisms (11-13). By contrast, we have shown here that treatment with 1 mg/kg acylated ghrelin after induction of reperfusion failed to improve several end-point measures of stroke outcome, with no significant reduction in infarct, swelling, or apoptosis (TUNEL or cleaved caspase-3 expression), and no improvement in neurological or motor performance. Similarly, even a 5-fold higher dose of acylated ghrelin had no beneficial effect on these measures of post-stroke outcome. Interestingly, the neuroprotective effects of acylated ghrelin in a mouse model of Parkinson's disease are dependent on metabolic status. Specifically, acylated ghrelin was neuroprotective when administered to fasted mice, whereas it had no effect during *ab libitum* feeding (29). Here, we studied mice that had been fed *ab libitum* prior to stroke surgery. However, food intake was markedly reduced after stroke induction (~90%), which is consistent with the tMCAo model of stroke (30). Thus, although the mice were fed *ab libitum* prior to stroke surgeries, there were in fact in a relatively 'fasted state' during the treatment regime. Notably, of the studies showing the protective actions of acylated ghrelin when administered pre-stroke, only one study detailed that rats were fasted overnight prior to surgery and acylated ghrelin administration (31), whereas the remaining studies did not describe whether there were fasted or fed *ab libitum* (11-13).

Although GHSR1a mRNA expression levels were decreased in ischemic hemispheres of vehicle-treated mice, levels in mice treated with acylated ghrelin were comparable to sham-operated mice, showing that post-stroke treatment up-regulates GHSR1a. Consistent with this, other studies have shown that peripheral administration of acylated ghrelin up-regulates GHSR1a expression (12, 32). However, the mechanisms underpinning this effect are

unknown. Nevertheless, our data indicate that down-regulation of acylated ghrelin's receptor does not account for its lack of effect on stroke outcome. Importantly, acylated ghrelin's appetite stimulating properties may be altered after stroke, actions that are largely mediated through the hypothalamus. Specifically, we found that acylated ghrelin had no effect on food intake by stroke mice during the treatment period, whereas it increased intake in sham controls. This finding raises the possibility of a generalized 'resistance' to acylated ghrelin in the acute period after stroke, which may extend to extra-hypothalamic brain regions involved in infarct development. An additional and plausible explanation for the apparent time-dependence of acylated ghrelin's protective effects could relate to its ability to more effectively prevent/inhibit mechanisms of ischemia-related injury than those caused by reperfusion (see discussion below). Irrespective of the reasons, our findings suggest that the timing of administration may be critical for acylated ghrelin's neuroprotective effects, casting doubts on it suitability for development as an acute stroke therapy.

Des-acylated ghrelin is structurally identical to the acylated form apart from the absence of a medium-chain fatty acid at serine position 3, which is essential for activity at GHSR1a (7). Despite this, des-acylated ghrelin often produces distinct biological effects to that of the acylated form. For example, we have recently shown that it exerts protective effects on cerebral arteries (e.g. suppressing Nox oxidase activity), whereas acylated ghrelin has no effect (16). In contrast to acylated ghrelin, post-stroke administration of des-acylated ghrelin was protective, with a marked reduction in both infarct and swelling at 24 hours, and an improvement in neurological and motor performance. In rodents, the vast majority (~70-80%) of the infarct volume development takes place during the first 24 hours (33). However, we cannot exclude the possibility that des-acylated ghrelin slowed the evolution of ischemic damage rather than reducing final infarct volume. Next we found evidence that this beneficial effect of des-acylated ghrelin was related to the degree of apoptosis in the ischemic hemisphere. Specifically, des-acylated ghrelin reduced the number of TUNEL-positive cells in peri-infarct regions, and prevented the increase in cleaved caspase-3 expression. Des-acylated ghrelin is known to directly protect neurons against ischemia-like conditions *in vitro* through anti-apoptotic mechanisms (15), thus it is likely that direct neuroprotective actions contribute des-acylated ghrelin's beneficial effect on infarct volume *in vivo*.

There is a growing appreciation of the importance of protecting the cerebral endothelium as part of an effective stroke therapy. Thus, we next tested the effects of the peptides on BBB

disruption *in vivo* and *in vitro*. Consistent with its lack of effect of stroke outcomes, acylated ghrelin had no beneficial effect on BBB permeability *in vivo* or the hyper-permeability of cerebral microvascular endothelial cells exposed to OGD + RO *in vitro*. This may relate, at least in part, to the lack of GHSR1a in the cerebral vasculature (16) and cerebral microvascular endothelial cells. Thus, it is highly improbable that acylated ghrelin modulates end-point measures of BBB disruption such as tight junction protein expression, cell viability, and apoptosis. Hence, we did not examine the effect of acylated ghrelin on these end-point measures in bEnd.3 cells exposed to OGD + RO. Des-acylated ghrelin on the other hand strongly protected against BBB hyper-permeability and thus BBB disruption *in vivo*. Moreover, it attenuated the hyper-permeability of cerebral microvascular endothelial cells when administered either before OGD or at the time of RO, inferring that direct effects on the cerebral endothelium contribute to its beneficial actions on BBB integrity *in vivo*. In accordance with the permeability data, des-acylated ghrelin prevented the loss of the tight junction protein occludin, increased levels of claudin-5, and appeared to reduce of ZO-1 re-distribution from the cell membrane to the cytosol. Des-acylated ghrelin also inhibited the death of cerebral endothelial cells exposed to OGD + RO, however, this occurred independently of a reduction in cleaved caspase-3 expression. The lack of effect of des-acylated ghrelin on cleaved caspase-3 expression is clearly in contrast to our earlier data showing that it markedly reduces expression levels in the ischaemic hemispheres of mice after stroke. It is conceivable that apoptotic pathways triggered in whole brain after ischaemia and reperfusion differ from those of cerebral microvascular endothelial cells. Thus, we presume that des-acylated ghrelin reduces death of bEnd.3 cells through caspase-3-independent anti-apoptotic pathways and/or necrotic cell death. Taken together, these data suggest that des-acylated ghrelin protects against BBB disruption by preventing the loss of tight junction integrity and by inhibiting endothelial cell death.

During early reperfusion, excess ROS/RNS formation by cerebral endothelial cells (and other cell types) triggers a number of downstream pathways that can directly mediate BBB disruption. Moreover, the Nox-NADPH oxidases are a significant source of ROS during reperfusion injury (4, 17, 18, 21, 34). Several lines of evidence indicate that des-acylated ghrelin may protect against BBB disruption by targeting these mechanisms. Firstly, des-acylated ghrelin has powerful ROS limiting properties in peripheral endothelial cells (35) and cerebral vessels (16). Indeed, we have shown that des-acylated ghrelin suppresses superoxide generation by cerebral arteries from ‘non-stroked’ mice via inhibition of the Nox oxidases.

Similarly, we have shown here that des-acylated ghrelin inhibited Nox activity in cerebral microvascular endothelial cells cultured under normoxic conditions. Secondly, des-acylated ghrelin attenuated OGD/RO-induced elevations in basal superoxide production by cerebral microvascular endothelial cells. Also, this was associated with reduced Nox activity, indicating an inhibitory action on the Nox oxidases. Lastly, des-acylated ghrelin decreased expression levels of 3-nitrotyrosine after OGD + RO, indicative of reduced peroxynitrite formation, the downstream product of the reaction between superoxide and NO. Taken together, these findings imply that the beneficial effects of des-acylated on BBB integrity and thus stroke outcome (in particular edema) involve a reduction in ROS/RNS generation by the cerebral endothelium as a result of Nox inhibition. Our previously published work (16) and data from this study indicate that unlike the des-acylated form, acylated ghrelin does not modulate ROS levels in cerebral vessels or inhibit cerebral vascular Nox oxidases. As such, this could be one possible reason why this ghrelin form is ineffective when administered during reperfusion, whereas des-acylated ghrelin strongly protects. Notably, Nox oxidases are also a major source of pathological ROS in endothelial cells of arteries upstream of the BBB, resident brain cells (e.g. neurons and microglia) and infiltrating leukocytes after stroke (4, 36). Des-acylated ghrelin could therefore improve stroke outcome by inhibiting the Nox oxidases in these cell types.

In summary, this study has revealed protective actions of des-acylated ghrelin when administered after initiating post-ischemic reperfusion, which involve a previously unrecognized beneficial effect on BBB integrity. Notably, we have shown previously that des-acylated ghrelin is a potent stimulator of vasodilator NO in cerebral vessels (16), and thus might also improve stroke outcome by supporting perfusion of the ischemic brain. Thus, taken together with its known direct neuroprotective actions (15), this study sheds light on the potential of des-acylated ghrelin (or longer-acting analogues, e.g. AZP-531 - currently in clinical trials for the treatment of obesity/type II diabetes) as a novel therapeutic agent that can target both neuronal and vascular mechanisms of ischemia/reperfusion-induced injury. Lastly, our findings may prove to be all the more crucial when we consider that its production may be reduced after stroke and in patients with stroke risk factors (37).

Disclosure/conflict of interest

The authors declare no conflict of interest.

Funding

This study was supported by a Project Grant from the National Health and Medical Research Council of Australia (NHMRC, APP1068442). We also acknowledge support from an Australian Postgraduate Award (JK), Australian Research Council Future Fellowships (FT 100109666 ZBA, SJS), and RMIT Vice-Chancellor's Senior Fellowships (AAM, SJS).

Author contribution statement

JMK acquired, analysed, and interpreted data relating to: 1) neurological and functional tests; 2) infarct and edema volumes; 3) TUNEL quantification; 4) BBB disruption *in vivo* and *in vitro;* 5) Western blotting for occludin and ZO-1; 6) cell death and superoxide production/Nox activity. MT acquired, analysed, and interpreted data relating to: 1) TUNEL experiments; 2) PCR for GHSR1a in the brain; and 3) immunofluorescence for ZO-1 and 3-nitrotyrosine. KYC acquired, analysed, and interpreted data relating to: 1) Western blotting analysis of caspase-3 expression in brain and bEnd.3 cells, and occludin in bEnd.3 cells. TB acquired, analysed, and interpreted data relating to PCR for GHSR1a in cerebral vessels and bEnd.3 cells. VA performed sham and stroke surgeries, and harvested tissue for associated experiments. JMK, MT, KYC, TB, and VA contributed to discussion, drafting of manuscript, and revision/approval of final version. CHYW, ZB & SJS contributed to the conception of the project, and revised/approved the final version of the article. AAM conceived and designed the study, performed stroke and sham surgeries, analysed and interpreted data, and drafted, revised, and approved the final version of the article.

References

1. Iadecola C, Anrather J. The immunology of stroke: from mechanisms to translation. Nature medicine. 2011;17(7):796-808.
2. Moskowitz MA, Lo EH, Iadecola C. The science of stroke: mechanisms in search of treatments. Neuron. 2010;67(2):181-98.
3. Gursoy-Ozdemir Y, Yemisci M, Dalkara T. Microvascular protection is essential for successful neuroprotection in stroke. Journal of neurochemistry. 2012;123 Suppl 2:2-11.
4. De Silva TM, Brait VH, Drummond GR, Sobey CG, Miller AA. Nox2 oxidase activity accounts for the oxidative stress and vasomotor dysfunction in mouse cerebral arteries following ischemic stroke. PloS one. 2011;6(12):e28393.
5. Palomares SM, Cipolla MJ. Vascular Protection Following Cerebral Ischemia and Reperfusion. Journal of neurology & neurophysiology. 2011;2011.
6. Gutierrez JA, Solenberg PJ, Perkins DR, Willency JA, Knierman MD, Jin Z, et al. Ghrelin octanoylation mediated by an orphan lipid transferase. Proceedings of the National Academy of Sciences of the United States of America. 2008;105(17):6320-5.
7. Andrews ZB. The extra-hypothalamic actions of ghrelin on neuronal function. Trends in neurosciences. 2011;34(1):31-40.
8. Gauna C, van de Zande B, van Kerkwijk A, Themmen AP, van der Lely AJ, Delhanty PJ. Unacylated ghrelin is not a functional antagonist but a full agonist of the type 1a growth hormone secretagogue receptor (GHS-R). Molecular and cellular endocrinology. 2007;274(1-2):30-4.
9. Delhanty PJ, Neggers SJ, van der Lely AJ. Mechanisms in endocrinology: Ghrelin: the differences between acyl- and des-acyl ghrelin. European journal of endocrinology / European Federation of Endocrine Societies. 2012;167(5):601-8.
10. Spencer SJ, Xu L, Clarke MA, Lemus M, Reichenbach A, Geenen B, et al. Ghrelin regulates the hypothalamic-pituitary-adrenal axis and restricts anxiety after acute stress. Biological psychiatry. 2012;72(6):457-65.
11. Hwang S, Moon M, Kim S, Hwang L, Ahn KJ, Park S. Neuroprotective effect of ghrelin is associated with decreased expression of prostate apoptosis response-4. Endocrine journal. 2009;56(4):609-17.
12. Miao Y, Xia Q, Hou Z, Zheng Y, Pan H, Zhu S. Ghrelin protects cortical neuron against focal ischemia/reperfusion in rats. Biochemical and biophysical research communications. 2007;359(3):795-800.

13. Zhou F, Xu J, Ying GY, Wang L, Zhu XD. Ghrelin attenuated cerebral ischemia reperfusion injury in rats. CNS neuroscience & therapeutics. 2012;18(11):945-6.
14. Chung H, Kim E, Lee DH, Seo S, Ju S, Lee D, et al. Ghrelin inhibits apoptosis in hypothalamic neuronal cells during oxygen-glucose deprivation. Endocrinology. 2007;148(1):148-59.
15. Chung H, Seo S, Moon M, Park S. Phosphatidylinositol-3-kinase/Akt/glycogen synthase kinase-3 beta and ERK1/2 pathways mediate protective effects of acylated and unacylated ghrelin against oxygen-glucose deprivation-induced apoptosis in primary rat cortical neuronal cells. The Journal of endocrinology. 2008;198(3):511-21.
16. Ku JM, Andrews ZB, Barsby T, Reichenbach A, Lemus MB, Drummond GR, et al. Ghrelin-related peptides exert protective effects in the cerebral circulation of male mice through a nonclassical ghrelin receptor(s). Endocrinology. 2015;156(1):280-90.
17. Radermacher KA, Wingler K, Langhauser F, Altenhofer S, Kleikers P, Hermans JJ, et al. Neuroprotection after stroke by targeting NOX4 as a source of oxidative stress. Antioxidants & redox signaling. 2013;18(12):1418-27.
18. Kahles T, Luedike P, Endres M, Galla HJ, Steinmetz H, Busse R, et al. NADPH oxidase plays a central role in blood-brain barrier damage in experimental stroke. Stroke; a journal of cerebral circulation. 2007;38(11):3000-6.
19. Brait VH, Jackman KA, Walduck AK, Selemidis S, Diep H, Mast AE, et al. Mechanisms contributing to cerebral infarct size after stroke: gender, reperfusion, T lymphocytes, and Nox2-derived superoxide. Journal of cerebral blood flow and metabolism : official journal of the International Society of Cerebral Blood Flow and Metabolism. 2010;30(7):1306-17.
20. Broughton BR, Brait VH, Kim HA, Lee S, Chu HX, Gardiner-Mann CV, et al. Sex-dependent effects of G protein-coupled estrogen receptor activity on outcome after ischemic stroke. Stroke; a journal of cerebral circulation. 2014;45(3):835-41.
21. Jackman KA, Miller AA, De Silva TM, Crack PJ, Drummond GR, Sobey CG. Reduction of cerebral infarct volume by apocynin requires pretreatment and is absent in Nox2-deficient mice. British journal of pharmacology. 2009;156(4):680-8.
22. Callaghan B, Furness JB. Novel and conventional receptors for ghrelin, desacyl-ghrelin, and pharmacologically related compounds. Pharmacological reviews. 2014;66(4):984-1001.

23. Harrison CB, Selemidis S, Guida E, King PT, Sobey CG, Drummond GR. NOX2beta: A novel splice variant of NOX2 that regulates NADPH oxidase activity in macrophages. PloS one. 2012;7(10):e48326.

24. Johnson SJ, Walker FR. Strategies to improve quantitative assessment of immunohistochemical and immunofluorescent labelling. Scientific reports. 2015;5:10607.

25. Miller AA, Drummond GR, Schmidt HH, Sobey CG. NADPH oxidase activity and function are profoundly greater in cerebral versus systemic arteries. Circulation research. 2005;97(10):1055-62.

26. Judkins CP, Diep H, Broughton BR, Mast AE, Hooker EU, Miller AA, et al. Direct evidence of a role for Nox2 in superoxide production, reduced nitric oxide bioavailability, and early atherosclerotic plaque formation in ApoE-/- mice. American journal of physiology Heart and circulatory physiology. 2010;298(1):H24-32.

27. Jackman KA, Miller AA, Drummond GR, Sobey CG. Importance of NOX1 for angiotensin II-induced cerebrovascular superoxide production and cortical infarct volume following ischemic stroke. Brain research. 2009;1286:215-20.

28. De Silva TM, Broughton BR, Drummond GR, Sobey CG, Miller AA. Gender influences cerebral vascular responses to angiotensin II through Nox2-derived reactive oxygen species. Stroke; a journal of cerebral circulation. 2009;40(4):1091-7.

29. Andrews ZB, Erion D, Beiler R, Liu ZW, Abizaid A, Zigman J, et al. Ghrelin promotes and protects nigrostriatal dopamine function via a UCP2-dependent mitochondrial mechanism. The Journal of neuroscience : the official journal of the Society for Neuroscience. 2009;29(45):14057-65.

30. Springer J, Schust S, Peske K, Tschirner A, Rex A, Engel O, et al. Catabolic signaling and muscle wasting after acute ischemic stroke in mice: indication for a stroke-specific sarcopenia. Stroke; a journal of cerebral circulation. 2014;45(12):3675-83.

31. Cheyuo C, Wu R, Zhou M, Jacob A, Coppa G, Wang P. Ghrelin suppresses inflammation and neuronal nitric oxide synthase in focal cerebral ischemia via the vagus nerve. Shock. 2011;35(3):258-65.

32. Zhang Q, Huang C, Meng B, Tang T, Shi Q, Yang H. Acute effect of Ghrelin on ischemia/reperfusion injury in the rat spinal cord. International journal of molecular sciences. 2012;13(8):9864-76.

33. Liu F, Schafer DP, McCullough LD. TTC, fluoro-Jade B and NeuN staining confirm evolving phases of infarction induced by middle cerebral artery occlusion. Journal of neuroscience methods. 2009;179(1):1-8.

34. Miller AA, Dusting GJ, Roulston CL, Sobey CG. NADPH-oxidase activity is elevated in penumbral and non-ischemic cerebral arteries following stroke. Brain research. 2006;1111(1):111-6.

35. Togliatto G, Trombetta A, Dentelli P, Gallo S, Rosso A, Cotogni P, et al. Unacylated ghrelin induces oxidative stress resistance in a glucose intolerance and peripheral artery disease mouse model by restoring endothelial cell miR-126 expression. Diabetes. 2015;64(4):1370-82.

36. Kahles T, Brandes RP. Which NADPH oxidase isoform is relevant for ischemic stroke? The case for nox 2. Antioxidants & redox signaling. 2013;18(12):1400-17.

37. Kantorova E, Chomova M, Kurca E, Sivak S, Zelenak K, Kucera P, et al. Leptin, adiponectin and ghrelin, new potential mediators of ischemic stroke. Neuro endocrinology letters. 2011;32(5):716-21.

Table 1. Summary of food intake prior to and after sham or stroke surgery

	Overnight food intake (grams)		
Experimental Group	**Baseline**	**24 h after surgery**	***n***
Vehicle			
Sham	3.5 ± 0.3	3.3 ± 0.4	*7*
Stroke	3.4 ± 0.7	0.35 ± 0.2*	*7*
Acyl ghrelin			
Sham	2.8 ± 0.4	4.9 ± 0.2$^{\#}$	*4*
Stroke	3.1 ± 0.38	0.32 ± 0.1	*4*

Values are given as mean ± SEM, where *n* = number of animals.

*$P<0.05$ vs. vehicle stroke baseline, and vehicle sham after surgery.

$^{\#}P<0.05$ vs. acyl ghrelin sham baseline.

Figure 1

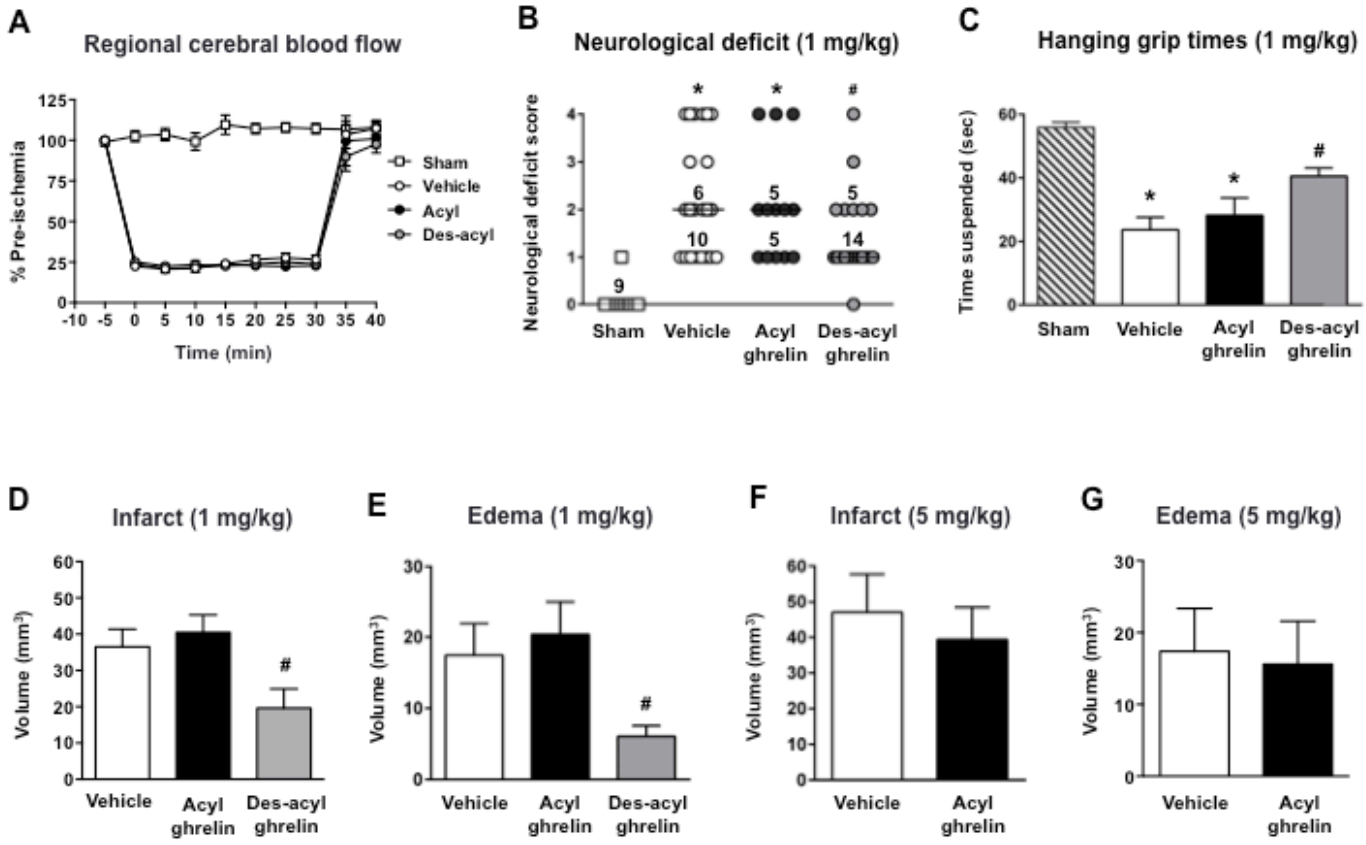
A
Regional cerebral blood flow
% Pre-ischemia
Time (min)
Sham
Vehicle
Acyl
Des-acyl
B
Neurological deficit (1 mg/kg)
Neurological deficit score
Sham
Vehicle
Acyl ghrelin
Des-acyl ghrelin
C
Hanging grip times (1 mg/kg)
Time suspended (sec)
D
Infarct (1 mg/kg)
Volume (mm³)
E
Edema (1 mg/kg)
F
Infarct (5 mg/kg)
G
Edema (5 mg/kg)

Figure 2

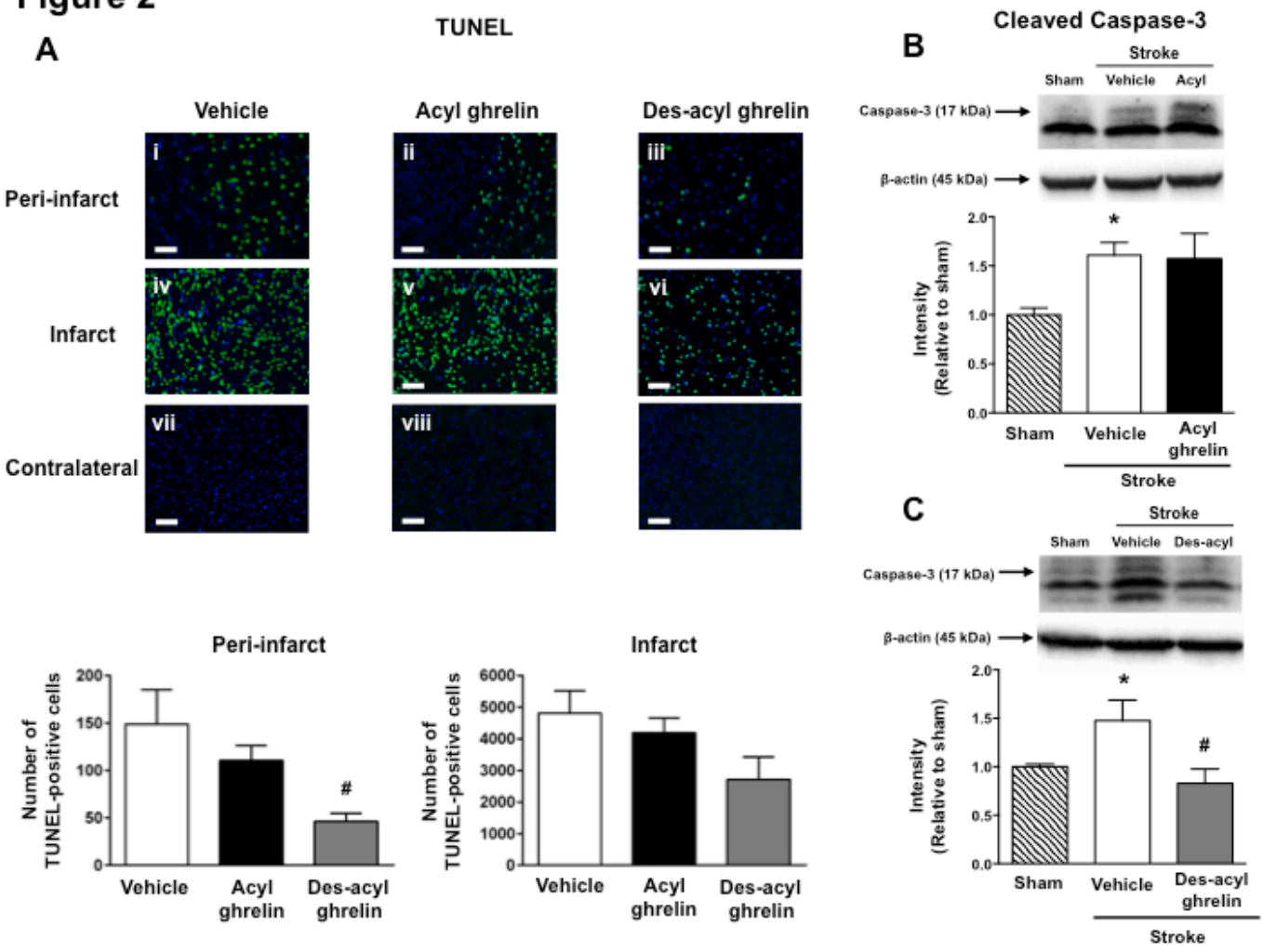
A
TUNEL
Vehicle
Acyl ghrelin
Des-acyl ghrelin
Peri-infarct
Infarct
Contralateral
i
ii
iii
iv
v
vi
vii
viii
Peri-infarct
Number of TUNEL-positive cells
Vehicle
Acyl ghrelin
Des-acyl ghrelin
#
Infarct
B
Cleaved Caspase-3
Stroke
Sham
Vehicle
Acyl
Caspase-3 (17 kDa)
β-actin (45 kDa)
Intensity (Relative to sham)
*
C
Des-acyl
#

Figure 3

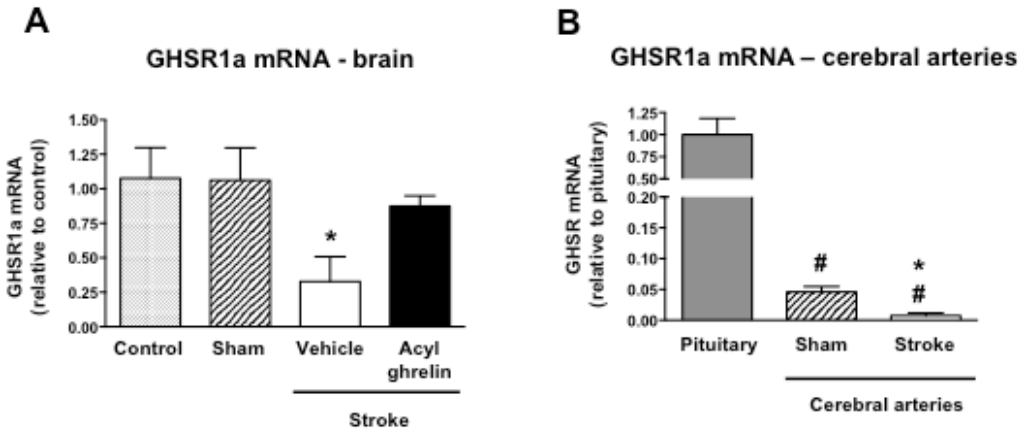
A
GHSR1a mRNA - brain
GHSR1a mRNA (relative to control)
1.50
1.25
1.00
0.75
0.50
0.25
0.00
*
Control
Sham
Vehicle
Acyl ghrelin
Stroke
B
GHSR1a mRNA – cerebral arteries
GHSR mRNA (relative to pituitary)
1.25
1.00
0.75
0.50
0.20
0.15
0.10
0.05
0.00
#
*
#
Pituitary
Sham
Stroke
Cerebral arteries

Figure 4

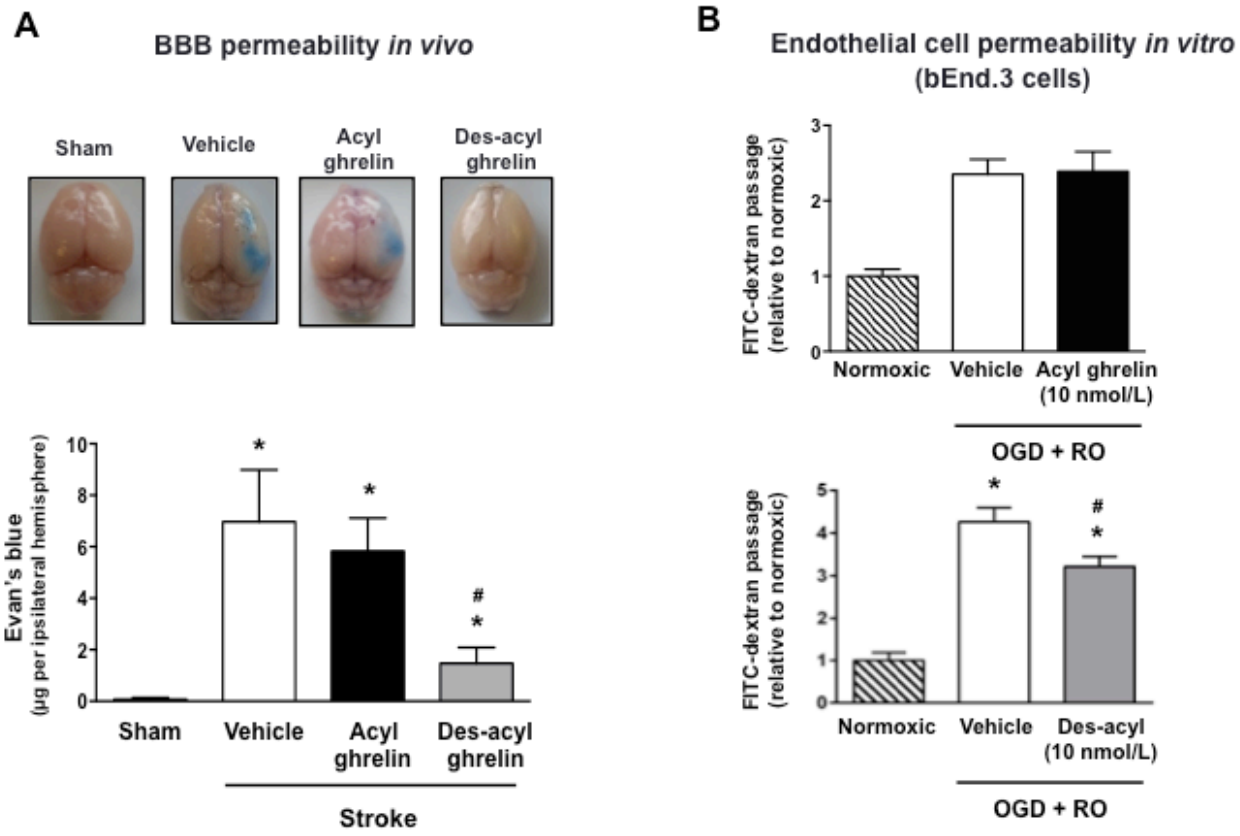
A
BBB permeability *in vivo*
Sham
Vehicle
Acyl ghrelin
Des-acyl ghrelin
Evan's blue (μg per ipsilateral hemisphere)
Sham
Vehicle
Acyl ghrelin
Des-acyl ghrelin
Stroke
B
Endothelial cell permeability *in vitro* (bEnd.3 cells)
FITC-dextran passage (relative to normoxic)
Normoxic
Vehicle
Acyl ghrelin (10 nmol/L)
OGD + RO
FITC-dextran passage (relative to normoxic)
Normoxic
Vehicle
Des-acyl (10 nmol/L)
OGD + RO

Figure 5

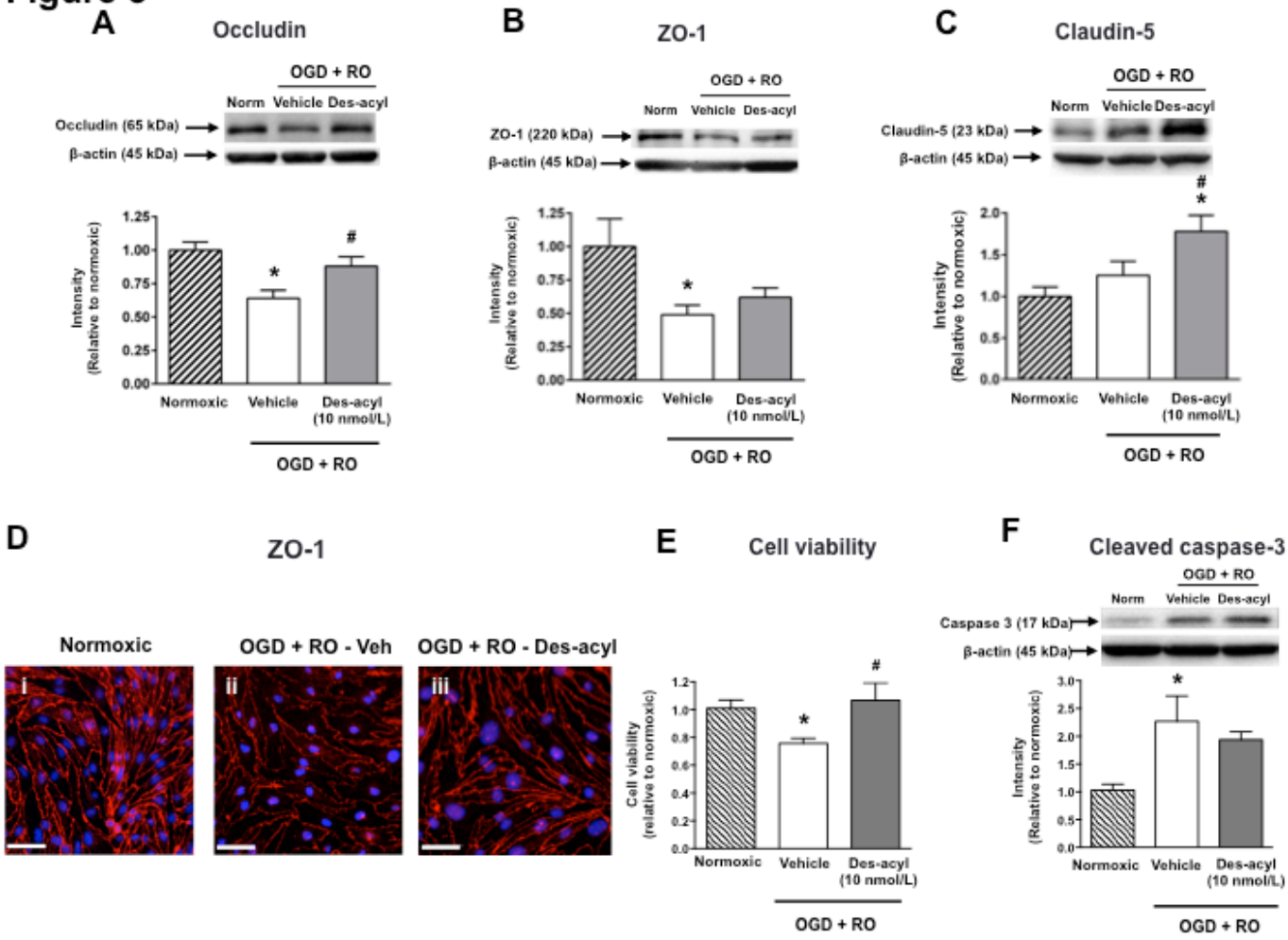
A
Occludin
OGD + RO
Norm
Vehicle
Des-acyl
Occludin (65 kDa)
β-actin (45 kDa)
Intensity (Relative to normoxic)
Normoxic
Vehicle
Des-acyl (10 nmol/L)
OGD + RO
B
ZO-1
ZO-1 (220 kDa)
C
Claudin-5
Claudin-5 (23 kDa)
D
ZO-1
Normoxic
OGD + RO - Veh
OGD + RO - Des-acyl
i
ii
iii
E
Cell viability
Cell viability (relative to normoxic)
F
Cleaved caspase-3
Caspase 3 (17 kDa)

Figure 6

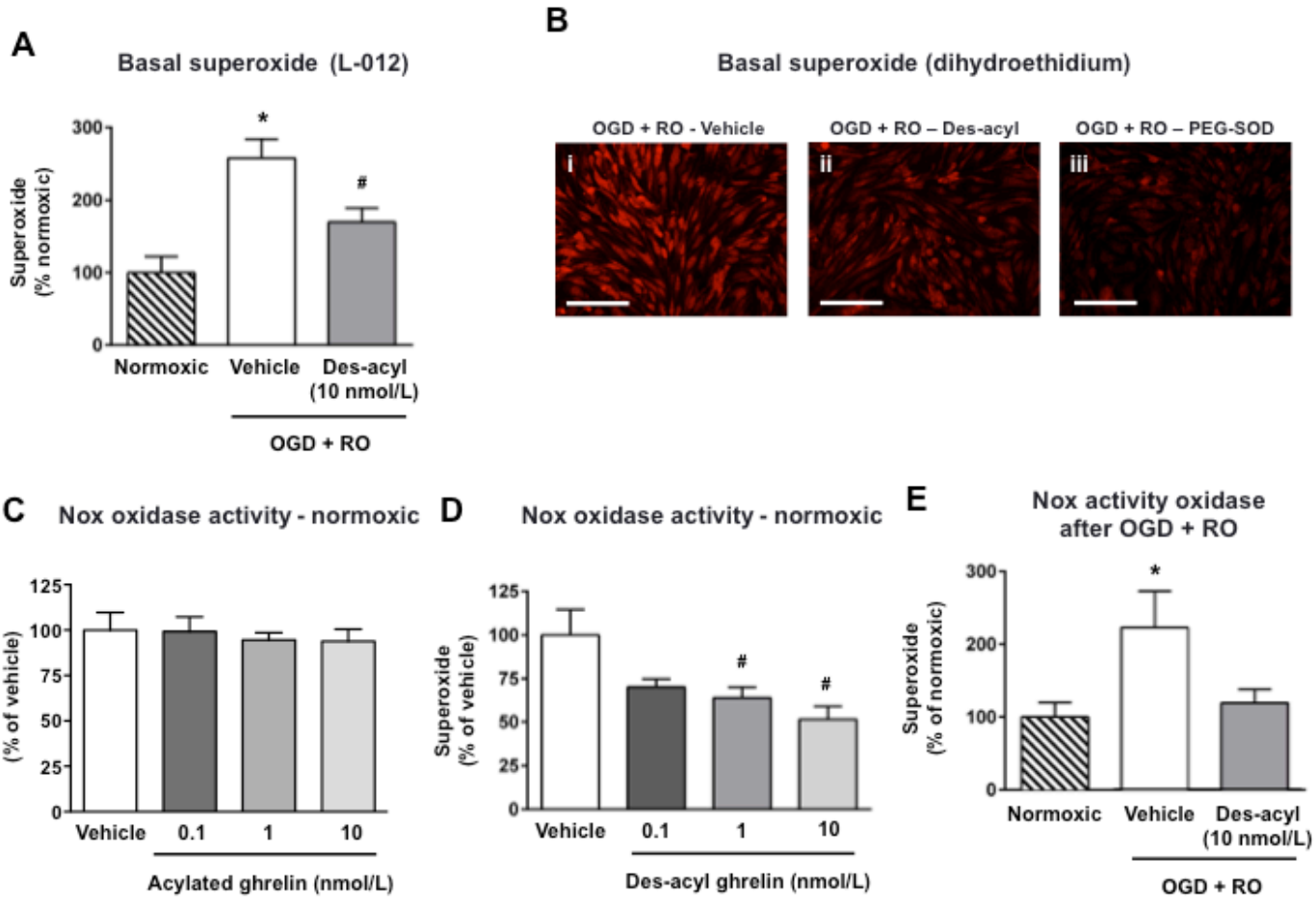
A
Basal superoxide (L-012)
Superoxide (% normoxic)
300
200
100
0
*
#
Normoxic
Vehicle
Des-acyl (10 nmol/L)
OGD + RO
B
Basal superoxide (dihydroethidium)
OGD + RO - Vehicle
OGD + RO – Des-acyl
OGD + RO – PEG-SOD
i
ii
iii
C
Nox oxidase activity - normoxic
Superoxide (% of vehicle)
125
100
75
50
25
0
Vehicle
0.1
1
10
Acylated ghrelin (nmol/L)
D
Nox oxidase activity - normoxic
Superoxide (% of vehicle)
125
100
75
50
25
0
#
#
Vehicle
0.1
1
10
Des-acyl ghrelin (nmol/L)
E
Nox activity oxidase after OGD + RO
Superoxide (% of normoxic)
300
200
100
0
*
Normoxic
Vehicle
Des-acyl (10 nmol/L)
OGD + RO

Figure 7

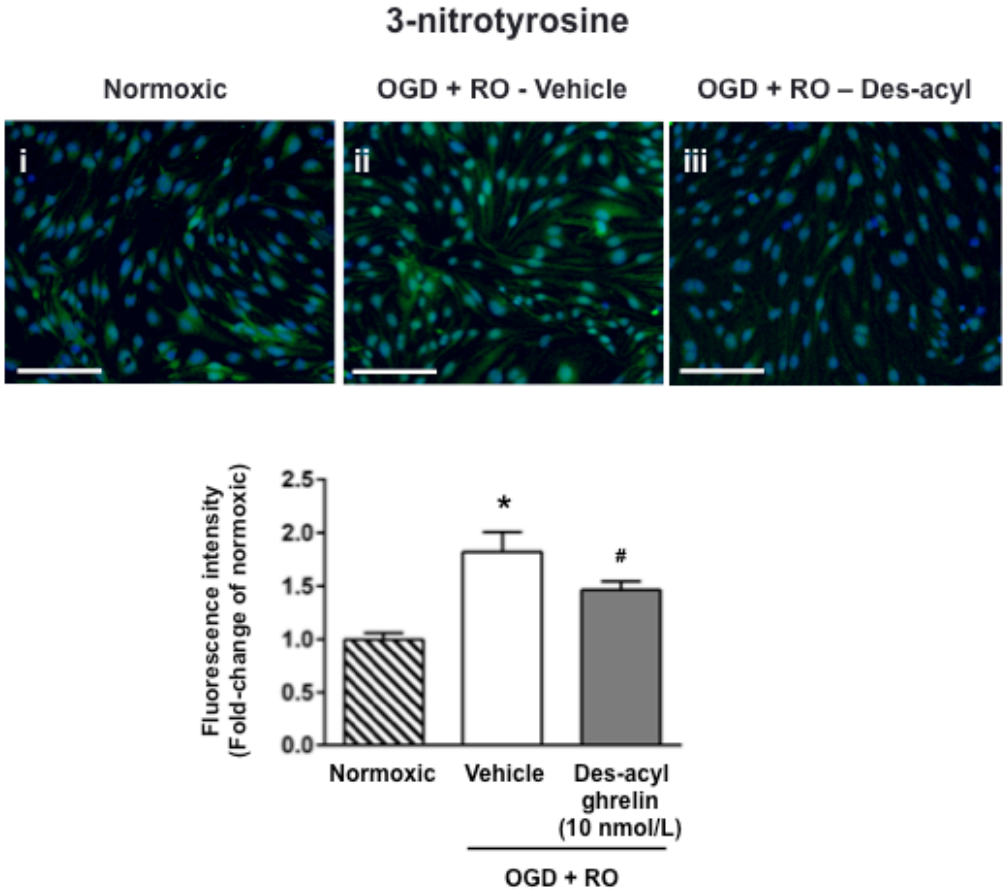
3-nitrotyrosine
Normoxic
OGD + RO - Vehicle
OGD + RO – Des-acyl
i
ii
iii
Fluorescence intensity
(Fold-change of normoxic)
2.5
2.0
1.5
1.0
0.5
0.0
*
#
Normoxic
Vehicle
Des-acyl
ghrelin
(10 nmol/L)
OGD + RO

Figure Legends

Figure 1. rCBF during sham (n=8) or stroke surgery (**A**, vehicle-treated [n=42]; acylated-treated [n=39]; des-acylated-treated [n=35]). Neurological deficit scores (**B**, sham: n=8; stroke: n=25 for all stroke groups), hanging wire times (**C**, sham: n=8; stroke: n=25 for all stroke groups), infarct (**D**, n=13 for all groups; **F**, n=10 for both groups) and edema volumes (**E**, n=13 for all groups; **G**, n=10 for both groups), 24 h after sham or stroke surgery. Stroke mice were treated with vehicle, acylated ghrelin (1 mg/kg or 5 mg/kg), or des-acylated ghrelin (1 mg/kg). Lines in **B** indicate median scores. Values in all other graphs are given as mean ± SEM. **P*<0.05 vs. sham mice, #*P*<0.05 vs. vehicle-treated mice (1-way ANOVA with a Dunnett's post-hoc test or Mann-Whitney U test).

Figure 2. A, Quantification of TUNEL-positive cells in peri-infarct and infarct brain regions 24 h after stroke in mice treated with vehicle (n=7; **i**, **iv**), acylated ghrelin (1 mg/kg, n=7; ii, v), or des-acylated ghrelin (1 mg/kg; n=7; iii, vi). Magnification = x10; scale bar = 100 μm. **B** & **C**, Representative Western blots and summary of band intensity for cleaved caspase-3 (17 kDa subunit) expression in ischemic/right cerebral hemispheres from mice 24 h after sham (n=9) or stroke surgery (vehicle; acylated ghrelin [1 mg/kg, **B**], des-acylated ghrelin [1 mg/kg, C], n=5-9). Values are given as mean ± SEM. **P*<0.05 vs. sham mice, #*P*<0.05 vs. vehicle-treated mice (1-way ANOVA with a Dunnett's post-hoc test).

Figure 3. A, GHSR1a mRNA expression in ischemic/right cerebral hemispheres of mice after sham (n=6) or stroke surgery (n=5) relative to expression levels in control mice (n=4). Stroke mice were treated with either vehicle or acylated ghrelin (1 mg/kg). **B,** GHSR1a mRNA in cerebral arteries of mice 24 h after sham or stroke surgery (untreated) relative to expression levels in the pituitary (positive control; n=4 for all groups). Values are given as mean ± SEM. **P*<0.05 vs. sham, #*P*<0.05 vs. pituitary (1-way ANOVA with a Dunnett's post-hoc test).

Figure 4. A, Quantification of BBB permeability 24 h after sham (n=6) or stroke surgery (vehicle; acylated ghrelin [1 mg/kg]; des-acylated ghrelin [1 mg/kg]; n=6 for all groups). **B**, Quantification of paracellular permeability of bEnd.3 cells after exposure to normoxic conditions or OGD + RO (n=6 for all groups). Cells were treated with either acylated ghrelin (top graph) or des-acylated ghrelin (bottom) at the time of RO (10 nmol/L). Values are given

as mean ± SEM. *P<0.05 vs. sham mice, #P<0.05 vs. vehicle-treated mice (1-way ANOVA with a Dunnett's post-hoc test).

Figure 5. Representative Western blots and summary of band intensities for tight junction protein expression (occludin [**A**, n=6], ZO-1 [**B**, n=6], and claudin-5 [**C**, n=4]) in bEnd.3 cells after exposure to normoxic conditions or OGD + RO. **D**, Representative photomicrographs of ZO-1 immunofluorescence (red) and nuclear staining with hoescht (blue) in bEnd.3 cells (n=3; **i**, normoxic; **ii**, vehicle; **iii**, des-acylated ghrelin [10 nmol/L]). Also shown is the effect of des-acylated ghrelin (10 nmol/L) on viability (**E**, n=5) and cleaved caspase-3 expression (**F**, n=5) in bEnd.3 cells after exposure to normoxic conditions or OGD + RO (n=5). Magnification = x40; scale bar = 50 μm. Values are given as mean ± SEM. *P<0.05 vs. normoxic controls, #P<0.05 vs. vehicle-treated cells (1-way ANOVA with a Dunnett's post-hoc test).

Figure 6. Effect of des-acylated ghrelin (10 nmol/L) on basal superoxide production by bEnd.3 cells after exposure to normoxic conditions or OGD + RO, as measured by L-012-enhanced chemiluminescence (**A,** n=9) or ethidium/oxyethidium fluorescence (dihydroethidium; **B,** representative of n=3). Also shown is the effect of des-acylated ghrelin (1-100 nmol/L) or acylated ghrelin on angiotensin II-stimulated superoxide production (**C**-**E**; Nox activity, n=9). Magnification = x40; scale bar = 100 μm. *P<0.05 vs. normoxic controls, #P<0.05 vs. vehicle-treated cells (1-way ANOVA with a Dunnett's post-hoc test).

Figure 7. Representative photomicrographs and semi-quantitative analysis of 3-nitrotyrosine immunofluorescence (green) and nuclear staining with hoescht (blue) in bEnd.3 cells after exposure to normoxic conditions or OGD + RO (**i**, normoxic; **ii**, vehicle; **iii**, des-acylated ghrelin [10 nmol/L]). All values are given as mean ± SEM (n=6). *P<0.05 vs. normoxic controls, #P<0.05 vs. vehicle-treated cells (1-way ANOVA with a Dunnett's post-hoc test). Magnification = x40; scale bar = 100 μm.